Density functional studies of structural and electronic properties of potassium alanate as a candidate for hydrogen storage

Samira Adimi[1], Hadi Arabi[1,*], Shaban Reza Ghorbani[1], Faiz Pourarian[2]

[1] Renewable Energies, Magnetism and Nanotechnology Research Laboratory, Department of Physics, Ferdowsi University of Mashhad
[2] Department of Materials Science and Engineering, Carnegie Mellon University, Pittsburgh, PA USA

Article Information

Abstract

Potassium Alanate has been one of the goal candidates for hydrogen storage during the past decades. In this report, the Density Functional Theory was initially applied to simulate the electronic and structural characteristics of the experimentally known $KAlH_4$ complex hydride. The relaxation of unit cell parameters and atomic positions was conducted until the total residual force was reduced to less than 0.001eV per unit cell. The final deduced cell parameters of this orthorhombic structure were a=8.834, b=5.763, c=7.328A°. Calculations were carried out by using the Projected Augmented Plane wave method via the QUANTUM ESPRESSO Package. In the next step, the Density of States calculations together with the band structure results showed that our data coincides with a non-magnetic $KAlH_4$ insulator with a band gap of 5.1eV. In order to investigate the nature of the chemical bonds in the crystal structure, the charge density distribution in (100), (010), (001), and (110) planes, along with the Born Effective charge and Löwdin population was used. The results show the transition of a partial charge from K^+ cation to $[AlH_4]^-$ subunit which leads to an ionic bond.

1. Introduction

Lack of an ideal storage material, especially in a practical and economical usage is the most significant challenge of on-board applications of hydrogen energy, and make it impractical for general use. Hydrogen can be stored in three different shapes: gaseous, liquid and inside the bulk of a solid-state material. However, storing it as a gas or liquid has several disadvantages such as occupying large volume and high cost. Up to now the storage of hydrogen in solid-state form seems to be the most preferable way. But candidate solid-state materials for this purpose have obstacles and difficulties.

The US Department of Energy (DOE) has set a target for an appropriate storage materialto 2017. This material should reach gravimetric 5.5Wt% H_2 and volumetric 40g/L [1] hydrogen absorption at temperatures between 40-85°C and pressure of 1bar. This leads toa formation energy in the range of -30 to -48kJ/mol H_2 [2] to meet the requirement condition for fuel-cell powered vehicles. However, no

*Corresponding Author's E-mail address: arabi-h@um.ac.ir

single material has met all these conditions yet and development of a high volumetric and gravimetric hydrogen storage material with fast dehydrogenation/ re-hydrogenation rate has been the subject of significant efforts in this technology during the past.

Among the wide range of available options for on-board hydrogen storage, metal complex hydrides have the potential to be used as an efficient materials due to their high purity of releasing H_2, light weight, low cost, easy accessibility, high hydrogen capacities ($NaAlH_4$ with a 7.5 wt. %, and $LiAlH_4$, $Mg(AlH_4)_2$ and $KAlH_4$ with 10.6wt%, 9.34wt% and 5.7wt%, respectively) and moderate decomposition temperature. Sodium and lithium alanates are commercial products, magnesium alanate usually synthesizes from sodium alanate, and MgH_2 and potassium alanate can be prepared under high pressure and temperature condition from potassium hydride and Al [3].

In recent years, sodium alanate has received a lot of interests-since Bogdanovic and Schwichard showed that it has a reversibility nature at moderate pressures and temperatures after adding titanium compound as a catalyst [4]. The reversible process of re/dehydrogenation happens in two step:

$$3NaAlH_4 \leftrightarrow Na_3AlH_6 + 2Al + 3H_2$$
$$Na_3AlH_6 \leftrightarrow 3NaH + Al + 3/2\ H_2$$
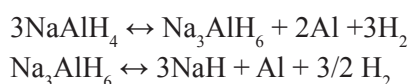
By modification of synthesis methods, the desorption temperatures in the presences of Ti-based catalysts was decreased to nearly 100℃ and 130℃ [5].

This discovery sparked a lot of interest in hydrides and a tremendous amount of research was done on the decomposition of $LiAlH_4$, which has the highest theoretically percentage of hydrogen (10.6wt %). Unfortunately, without the presence of any doping catalyst the dehydrogenation of this material requires more than 400°C and a pressure above 10000 bar [6]. Therefore, this compound definitely is not suitable for transport purpose. Adding a suitable doping catalyst will significantly lower the pressures and temperatures [7, 8] but not as much as needed. The exact reaction mechanism of alanates with hydrogen and the role of

additives are not yet fully understood, and is the major problem in theoretical studies of complex hydrides.

Potassium alanate has a structure very similar to lithium and sodium alanates, but experimental reports show a main advantage for $KAlH_4$. It has the reversibility of hydrogen without any need for an additional additive, at moderate temperatures (250-300°C) and low pressures (<1MPa).

Numerous experimental and theoretical studies indicate that the decomposition reaction of alanates passes through a stable intermediate phase, with the formula of M_3AlH_6 (M=Na, Li, ...) [5,7]. Despite these reports, Arnbjerg and Jensen observed three intermediate phases during the de/rehydrogenation of potassium alanate but none of them have the monoclinic structure of K_3AlH_6 [9]. The formation of each phase depended on the different mechanical and chemical preparation processes, another effort by Pukazhselvan et al. done recently revealed the K_3AlH_6 phase during the decomposition of potassium alanate was not successful [5]. This is another factor to distinguish potassium alanates from other alanates of its family.

Nevertheless, the main obstacle for practical application of $KAlH_4$ is the slow dehydrogenation kinetics of hydrogen reflected in the high pressure and temperature of its forward and reverse processes [10].

Few theoretical studies have been done to understand the structural properties of $KAlH_4$. First, Hiroyuki Morioka et al. tried to predict the crystal structure and thermochemistry of potassium alanates [11], then Vajeeston et al. considered seven close structural types [12] to predict the ground structure of $KAlH_4$ by applying a DFT calculation implemented with Vienna ab initio simulation package (VASP) [13] to show that an orthorhombic structure with a $KGaH_4$-type form has the minimum total energy among others.

Understanding the mechanism of catalyst-free reversibility in $KAlH_4$ might guide us in obtaining similar improvement with other alanates. Furthermore, we can look at this material as a model system to understand hydrogen storage formalism, to design new materials for hydrogen storage with improved

weight-percentage of hydrogen, and to try and find better catalysts which may result in speeding up the kinetics of the reaction.

However, finding the crystal structure of potassium alanate by experimental methods is not easy. The reasons related to the low scattering power of hydrogen for obtaining hydrogen positions by using X-ray diffraction [14], difficulty of synthesizing sufficiently large crystals [5] and the usual structural complexity of hydrides [12].

Motivated by this subject, in this study we reported crystal, electronic structures, heat of formation of $KAlH_4$ and electron charge density using the Density Functional Theory (DFT) calculation method, which exhibits an insulator characteristic with a calculated energy band gap of 5.01 eV. Moreover, using the Born Effective charge calculation the ionic characteristic between K and $[AlH_4]$, where about one electron is transferred from K to $[AlH_4]$ block, is obvious.

2. Computational methodology

Our calculations for structural relaxation and electronic properties were performed based on the Density Functional Theory (DFT) [15] in a basis set of plane waves as implemented in the Quantum Espresso Package [16]. The electron-core interactions were placed on the Projector Augmented Wave (PAW) pseudo-potentials [17] for all our Pw-PP calculations. The atomic valence electrons are $3s^2 3p^1$, $1s^1$ and $3s^2 4s^1 3p^6$ for Al, H and K, respectively [18]. For our initial presumptive values we used an orthorhombic unit cell with a Pnma space group determined by X-ray diffraction pattern by Joes R. Ares et al. [10] at room temperature. Then the structure was fully relaxed by allowing both ionic positions and lattice parameters to be changed, until the residual forces on each atom were less than 10^{-3} eV. The cutoff energy was 40 Ry in all calculations and a 6×8×6 k-point mesh, generated by the Monkhorst Pack method [19], was used to sample the first Brillouin zone. Convergence threshold (criterion) of self-consistent energy was less than 10^{-4} a.u per unit cell and the Broyden–Fletcher–

Goldfarb–Shanno (BFGS) quasi-Newton algorithm [20] was used to calculate the ground state geometry of the structure. The Density of States (DOS) was determined by applying the tetrahedron integration method [21] and the projection of calculated wave functions over orthogonalized atomic pseudo-orbitals (corresponding to the occupied valence electron shells) enabled us to calculate the Partial density of States (PDOS).

3. Results and discussion

3.1. Structural properties

The optimized geometry of complex hydride $KAlH_4$ is shown in Figure 1. This relatively light alanate is crystallized in the orthorhombic structure with the lattice parameter of a=8.834, b=5.763, c=7.328A˚. The lattice parameters and its cell volume are compared with the experimental results [10, 11] in Table 1. The calculated unit cell at zero temperature is in good agreement with that of the experimental work. Furthermore, we present and compare our simulated results with that of some previous theoretical works in Table 2 [12, 22] which clearly shows coincident values. Due to the absence of total energy in the references, we also calculated the total energy of their reported structures using the Quantum Espresso Package (presented in the fourth column of Table 2) and found that our relaxation procedure resulted in a structure with lower energy. The positions of K, Al and H atoms in $KAlH_4$ have been calculated and are reported in Wyckoff notation in Table 3.

The relax structure has slightly distorted $[AlH_4]^-$ blocks, which are separated by K^+ cations as shown in Figure 2. The ionic size of K^+ is 1.33A˚ and the distance of Al-H bonds vary between 1.627-1.637 A˚. Each Potassium ion is surrounded by 12 atoms of Hydrogen whose distances changed from 2.667 to 4.982 A˚.
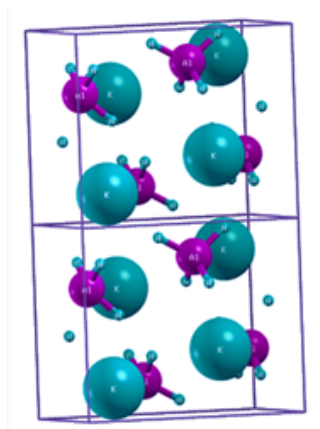
Fig. 1. The Crystal structure of KAlH$_4$. Aluminum atoms are purple spheres in construct with Hydrogen in [AlH$_4$]$^-$ blocks.

3.2. Electronic properties

Investigation of the electronic properties of alanates, especially the distributions of the Density of available States and band structure, could be used as a key method for basic and advanced studies on their structural and hydrogen storage properties.

The total Density of States (DOS) of KAlH$_4$ and partial electronic DOS for each atomic species (K, Al, H) in the optimized structure are plotted in Figure 3. The Fermi level is set at zero energy. In all partial DOS plots s-states are shaded, 3s^1 states of Potassium are dotted, and the p states are presented without any marks.

Table 1. Comparison of calculated and experimental values of the unit cells of KAlH$_4$.

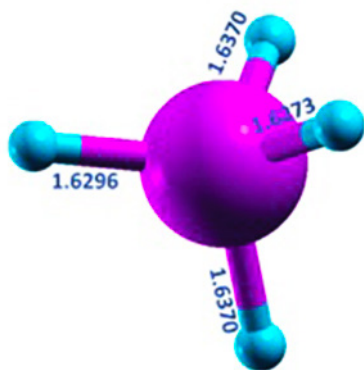| a(Å)	b(Å)	c(Å)	Cell volume	References
8.858	5.822	7.352	378.15	10
8.8515(14)	5.8119(8)	7.3457(5)	377.89	9
8.834	5.763	7.328	373.07	This work

Fig. 2. The distorted AlH$_4$ Block with negative charge.

From these plots it is obvious that the valence band in total DOS is mainly derived from s and p orbitals of aluminum and s the orbital of hydrogen, and the conduction band is occupied by Al and K orbitals. Quite separation of Al-s and Al-p states is clear from the projected DOS of Al, but these states are energetically mixed in the projected DOS of Potassium. Since the Al-p and H-s states are in the same range of energy, they are extremely suitable to form a hybridized sp orbitals and have a covalent bond which could lead to the formation of a [AlH$_4$]$^-$ group. It was revealed that the potassium states have a dominant contribution in its conduction bands and the contribution of an outer s-orbital of potassium

Table 2. Comparison of calculated unit cells and total forces with previous theoretical values.

a(Å)	b(Å)	c(Å)	Escf	Total Force	References
9.009	5.767	7.399	-629.0487	0.108	12
8.814	5.819	7.331	-629.0709	0.044	22
8.834	5.763	7.328	-629.0738	0.001	This work

Table 3. Optimized atomic position of KAlH$_4$ in Wyckoff notation. The Löwdin charges in last column, show valance electronic charges on each of the atom.

Atom	site	Positions			Löwdin Charge
Al	4c	0.5694	0.250	0.8196	2.81
K	4c	0.1778	0.250	0.1621	8.13
H	4c	0.4071	0.250	0.9247	1.25
H	4c	0.7121	0.250	0.9604	1.25
H	8d	0.5815	0.4783	0.6882	1.23

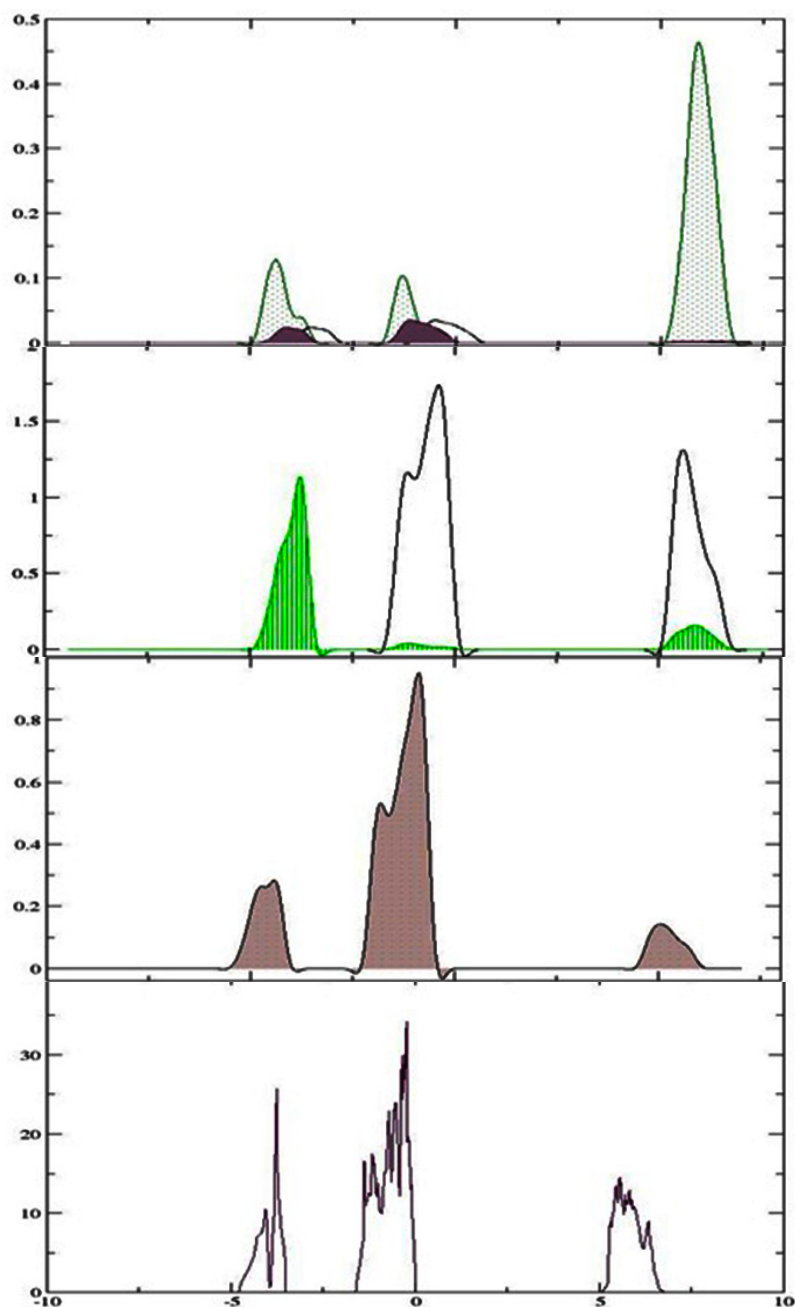**Fig. 3. Calculated DOS and the Projected DOS for Valence band of KAlH$_4$. The s-states are shaded and the 3s^1 in PDOS of K is dotted. The simple diagrams in the first two lines are p-states and the last diagram shows total Density of States. The Fermi energy is set to zero in all diagrams.**

in the valence band is very small, thus we expect a non-covalent interaction between the K and AlH$_4$ blocks. By comparison of total DOS of potassium in the elemental form with that of the KAlH$_4$ complex hydride, it can be seen that each K atom donates its electrons to the [AlH$_4$]$^-$ blocks and forms a cation ion. The total DOS shows the insulator behavior of potassium alanate with an energy gap of 5.19 eV. The main contribution of the peak with -2 to zero eV energy comes from the s orbital of hydrogen and p orbital of aluminum and the next peak, with almost -3.5 to -5 eV energy, arises from the contribution of the s orbitals of Al and H.

Figure 4 shows the calculated band structure along high symmetry directions Γ(0,0,0) to R(0.5,0.5,0.5). We know that there is a dependency of electronic energy to k-vectors, especially along high symmetry directions in the Brillouin zone, which gives us interesting information such as optical absorption and band gap of the materials which can be deduced from band structure plots [18]. Close to the Fermi energy level, there are flat bands in this plot which lead to a sharp peak in the total DOS of material. At Γ point the difference between valance bands and conduction bands is 5.02 eV which can be a good estimation of the KAlH$_4$ bandgap.

3.3. Born effective charge and Löwdin Population Analysis

The amount of electronic charge on each atom can be calculated with the help of Löwdin population analysis [23]. The extended plane-waves states of valence electrons would be projected on the psudo-atomic basis and the sum of these projections regarded as the Löwdin Charge.

For our considered pseudo-potential function, the free K and Al atoms have 3p^6 3s^2 3s^1 and 3s^2 3p^1 valence electron occupancies, respectively. The total Löwdin charge reported in Table 3 is the total valence charges of atoms in the complex hydride structure, so the charge on potassium and aluminum is 0.86 and 0.19 with a positive sign. On the other hand, H has a negative charge of -0.25 which makes the [AlH$_4$] group end up with a negative charge of -0.77e. The amount of charge on each atom is not a quantum mechanical observation, so these charges are a qualitative estimate, and since the Löwdin analysis tends to underestimate partial electronic charges only the signs and orders of the resulting numbers are noticeable. Anyway, it is clear that about one electron is transferred from K to the [AlH$_4$] group, so we will end up with an ionic bond.

The modern theory of polarization [24] calculates macroscopic polarization of the crystal using the Berry Phase approximation [25], which enables us to calculate the Born Effective Charge (BEC). BEC is a useful tool to determine electronic field polarization, derived on the bases of the linear response method via the ab-initio technique. It is defined as the response of the dipole moment of the system to displacement of a specific atom. When one of the ionic atoms is
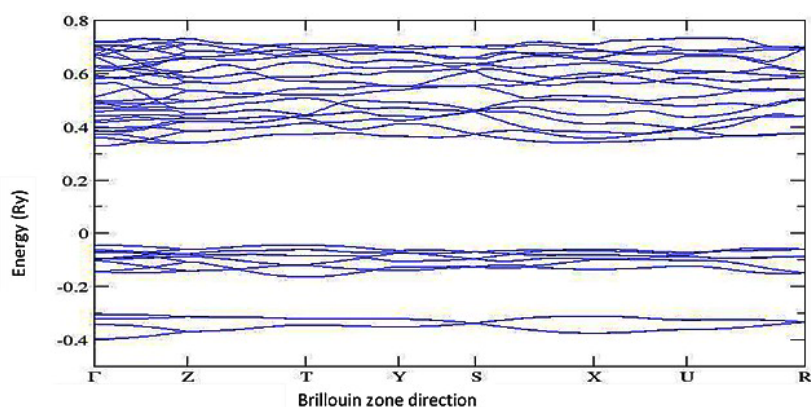

Fig. 4. Band Structure of KAlH$_4$ in the specific direction. The clearly shows insulator characteristic with a band gap of 5.02 eV.

displaced from its equilibrium position, the finite dipole moment of P can be computed using the Berry Phase approach: $Z_{i,j}^* = \Omega \, dp_i/dr_j$, where i and j are the Cartesian indices, Ω is the volume of the unit cell, P_i is the total polarization in the direction i, dr_j is the displacement of the specified atom and Z^* is the BEC with nine tensor compounds. The interest brought to this type of partial charge calculation is related to the quantum mechanical observation characteristic of the dipole moment which makes BEC stands out from either the Löwdin or Mulliken Population analysis [26] both of which rely on the charge of each atom.

The results provided in Table 4 show a diagonal tensor for K and Al atoms, but in contrast the BEC of hydrogen makes two different types of matrices, an asymmetric non-diagonal tensor for 8d and two diagonal tensor for 4c sites. The dynamical charges of H differ from -0.56e to -0.71e which is very close to its nominal charge. In general, the distribution of effective charge shows the ionic interaction between K atoms and hydrogen in the AlH_4 group and the charge concentration on H sites in the subunit.

ambient pressure to 200 bars. According to our simulation, there was no transition under pressure for the $KAlH_4$ ground state structure, which indicates the structure is stable under even higher pressures.

3.5. Charge density and Electron Localization Function (ELF)

In order to improve our understanding about the ionic and covalent nature of K-Al-H bonds, electron (pseudo-) charge density and difference charge density (crystal charge density minus the superposed atomic densities) are plotted in two dimensions for (100), (010), (001), (011), (101) and (110) planes (shown in Figure 5). The (110)-plane is the orientation with some K, Al and H atoms inside or close to the plane. The contour plot for charge density for this plane is shown in Figure 6.a. According to this result, a remarkable charge density is distributed between Al and H, indicating that they form an AlH_4 structural subunit and the partial ionic bond between them could not be a dominant one. On the other hand, there isn't any significant

Table 4. Born Effective Charges. The tensor is diagonal for Al and K but the H-8d tensor is an asymmetric one which shows low symmetry in contrast with Al and K.

Atom	Site	Z_{xx}	Z_{yy}	Z_{zz}	Z_{xy}	Z_{xz}	Z_{yx}	Z_{yz}	Z_{zx}	Z_{zy}
K	4c	1.24	1.22	1.17	0.0	0.03	0.0	0.0	0.0	0.0
Al	4c	1.27	1.23	1.28	0.0	0.0	0.0	0.0	0.07	0.0
H	4c	-0.66	-0.58	-0.66	0.0	-0.09	0.0	0.0	0.11	0.0
H	4c	-0.77	-0.58	-0.66	0.0	0.22	0.0	0.0	-0.09	0.0
H	8d	-0.56	-0.71	-0.61	0.01	0.01	0.0	-0.21	0.04	-0.24

3.4. Crystal structure under pressure

The effect of pressure on a material will shorten its crystal constants and interatomic distances which may cause changes in the chemical and physical properties of solid [27]. Since the potassium alanate structure in the α-$NaAlH_4$-type and $KGaH_4$-type ground state phases are energetically very close to each other, we performed a high pressure simulation to figure out whether the α-$NaAlH_4$-type arrangement would be a metastable state under specific pressures.

The range of pressure was set to be changed from

charge density distribution between K and AlH_4 unit. It is valuable to have a comparison between the charge density of potassium alanate and those of calcium and magnesium alanates as reported by Lovvik et al. through a similar plane [28]. In these three plots, there is a remarkably large charge distribution around the Alkali-earth atoms, but the more spherical symmetry around Ca atoms reflects more localization of Ca core electrons which may be interpreted as more stability of calcium alanate compared with potassium and magnesium alanates. The clear charge continuity among the atoms of $KAlH_4$ reflects its nearly layered

structure, which is a less layered configuration than $Mg(AlH_4)_2$, and on the other hand it is more planar than $Ca(AlH_4)_2$ [28].

stands for "simple measure of electron localization in atomic and molecular systems" [29]. It is an instructive measure of the electron localization to diagnose the
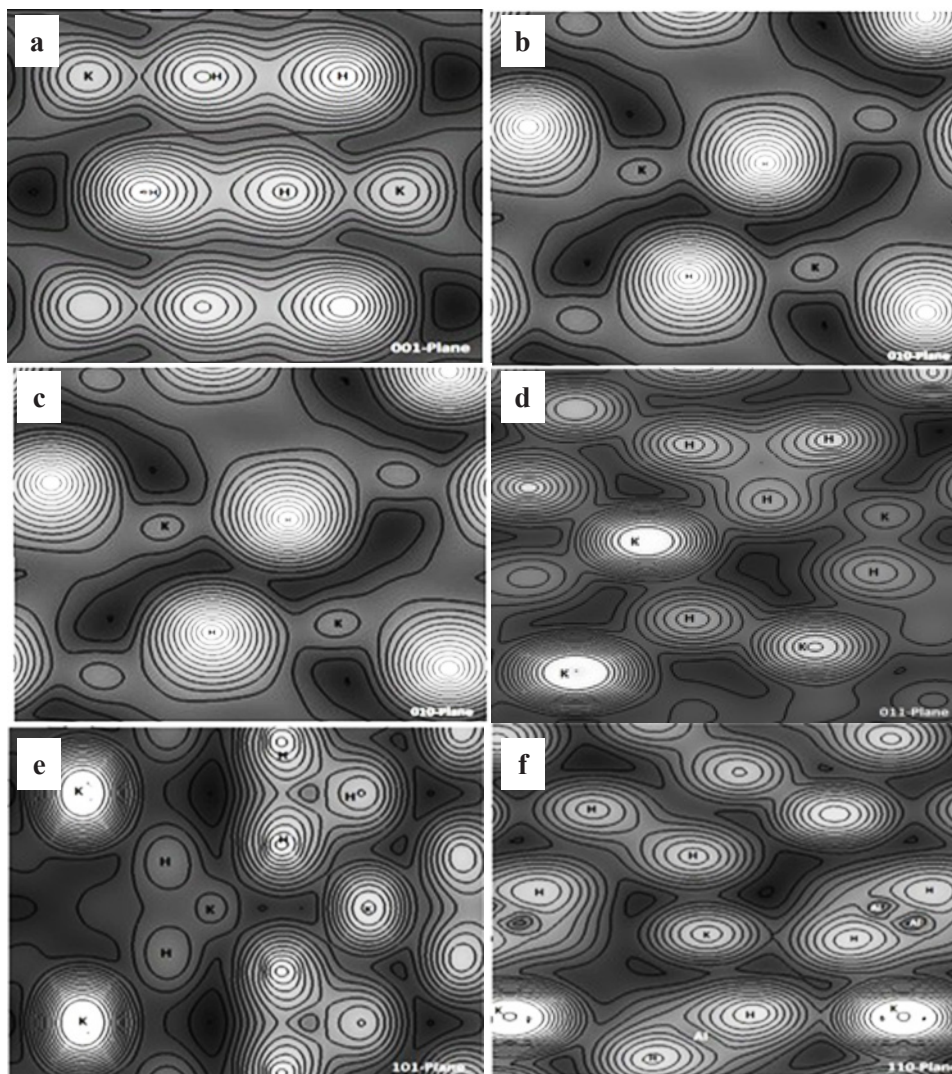

Fig. 5. Valence Charge Density in different planes. a) (001) surface, b) (010) surface, c) (100) surface, d) (011) surface, e) (101) surface, f) (110) surface

The charge transferred from K to the negative block is clear from the difference charge density distribution plotted in Figure 6.b. The positive values in the plot of transferring electronic charge corresponds to the excess of electron charge, and the negative values reflect the electron deficit. According to this image the charge transfer from Al to H is not isotropic, indicating that the bonding between Al and H could be categorized as an iono-covalent one.

In 1990, Becke and Edgecombe introduced ELF which

nature of chemical bonding in solids and its value is defined between 0-1. High values of ELF demonstrate paired electrons with covalent bonds. In Figure 6.c the ELF of potassium alanate in the (110) plane is shown. At first glance, we notice that AlH_4 produces a molecular-type subunit. The charge distribution around H atoms do not have a complete spherically symmetric and it is polarized toward aluminum atoms. The ELF continues within the AlH_4 block indicating the covalent bond between Al and H. Moreover,
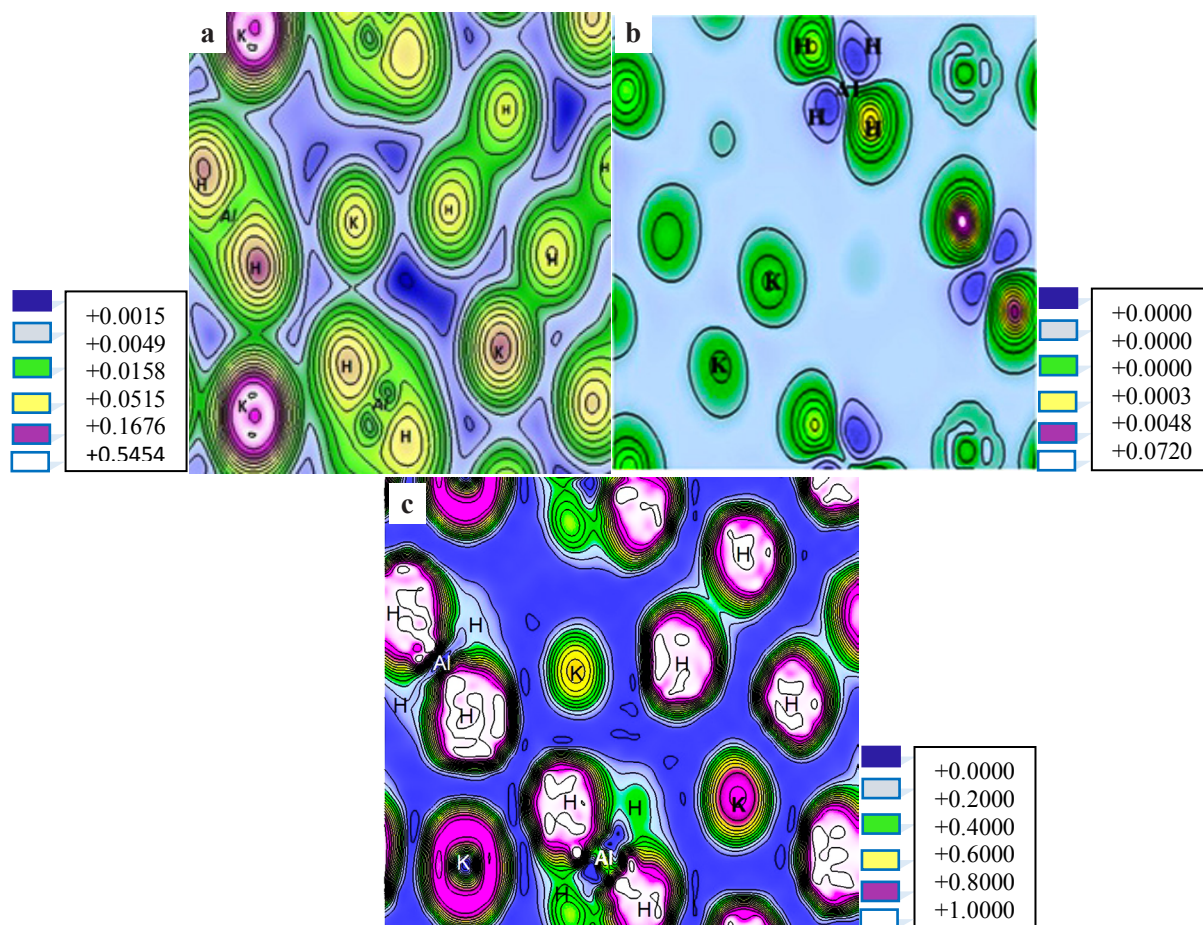
Fig. 6. (a) Valance Charge density (b) The difference charge density (c) Electron Localization densities map of KAlH₄-(110) surface. The ELF is normalized between 0 (for zero localization) and 1 (for complete localization).

the electron distributions around H atoms are quite localized, which points out the Boson-like behavior of electron pairs in these sites, while the Al atoms are surrounded with nonlocalized atoms. The ELF around the K atoms has a spherically symmetric distribution, and the ELF between K and H atoms is negligible. However, an independent ELF between K atoms and AlH₄ units is formed.

Briefly, the charge investigation also shows quite purely ionic bonding between K atoms and negatively charged [AlH₄]⁻ groups in agreement with aforementioned DOS and Band structure plots.

properties of KAlH₄ have been simulated using the DFT method within a PP-PW approach via the QUANTUM ESPRESSO package. Our calculated structural parameters are in good agreement with experimental results. Moreover, the band structure of KAlH₄ indicated that this material is an insulator with a band gap of 5.1eV at Gamma point. Considering the DOS plot, charge electronic density, and Born effective charge it was indicated that a K atom acts as a donor to form a cation ion and Al-H bonds have a covalent nature; therefore, an ionic bonding between K⁺ and the negatively charged [AlH₄]⁻ block will be predictable.

4. Conclusions

In this investigation, the structural and electronic

5. References

[1] U.S. Department of Energy, http://www1.eere.energy. gov/hydrogenandfuelcells/storage/pdfs/targets_onboard_ hydro_storage_explanation

[2] Schlapbach, L.; Zuttel, A. Hydrogen-Storage Materials for Mobile Applications. Nature, 2001, 414: 353.

[3] I.P. Jain, Pragya Jain, Ankur Jain, Novel hydrogen storage materials: A review of lightweight complex hydrides, Journal of Alloys and Compounds, 2010, 503: 303.

[4] Bogdanovic, B. & Schwickardi, M. Ti-doped alkali metal aluminium hydrides as potential novel reversible hydrogen storage materials. J. Alloys Compounds, 1997, 253:1.

[5] D. Pukazhselvan, Duncan Paul Fagg, O.N. Srivastava, One step high pressure mechanochemical synthesis of reversible alanates $NaAlH_4$ and $KAlH_4$, Int. J Hydrogen Energy, 2015, 40:4916.

[6] Mikheeva, V. I.; Troyanovskaya, E. A. "Solubility of Lithium Aluminum Hydride and Lithium Borohydride in Diethyl Ether". Bulletin of the Academy of Sciences of the USSR Division of Chemical Science, 1971, 20 (12): 2497.

[7] Lei Zang; Jiaxing Cai; Lipeng Zhao; Wenhong Gao; Jian Liu; Yijing Wang, Improved hydrogen storage properties of $LiAlH_4$ by mechanical, J. Alloys Compd., 2015, 647: 756.

[8] Chia-Yen Tan; Wen-Ta Tsai, Catalytic and inhibitive effects of Pd and Pt decorated MWCNTs on the dehydrogenation behavior of $LiAlH_4$, 2015, Int. J Hydrogen Energy, 40:10185.

[9] Lene Mosegaard Arnbjerg, Torben R. Jensen , New compounds in the potassium-aluminium-hydrogen system observed during release and uptake of hydrogen, Int. J. Hyd. Energy, 37, 2012: 345.

[10] Jose R. Ares; Aguey-Zinsou, K.; Leardini, .F.; Jımenez Ferrer, I.; Fernandez, J.; Guo, Z.; Carlos Sanchez J., "Hydrogen Absorption/Desorption Mechanism in Potassium Alanate ($KAlH_4$) and Enhancement by $TiCl_3$ Doping", Phys. Chem. C, 2009, 113: 6845.

[11] Morioka H., Kakizaki K., Sai-Cheong Chung, Yamada A., Reversible hydrogen decomposition of $KAlH_4$, J. Alloys Compd., 2003, 353: 310.

[12] Vajeeston, P., Ravindran, P., Kjekshus, A., Fjellvåg, H., Crystal structure of $KAlH_4$ from first principle calculations, J. Alloys Compd., 2004, L8: 363.

[13] G. Kresse, J. Hafner, Phys. Rev. B 47 (1993) R6726; G. Kresse, J. Furthmuller, Comput. Mater. Sci. 1996, 6:15

[14] Hai-Chen Wang, Jie Zheng, Dong-Hai Wu, Liu-Ting Wei, Bi-Yu Tang, Crystal feature and electronic structure of novel mixed alanate $LiCa(AlH_4)_3$: a density functional theory investigation, RSC Adv., 2015, 5: 16439.

[15] Hohenberg, Pierre; Walter Kohn, "Inhomogeneous electron gas". Physical Review, 1964, 136 (3B): B864

[16] P. Giannozzi, et al., J.Phys.:Condens.Matter, 2009, 21, 395502 http://dx.doi.org/10.1088/0953-8984/21/39/395502.

[17] Blochl PE., Projector augmented-wave method, Phys Rev B, 1994, 50:17953.

[18] We used the Pseudopotentials K.pbe-spn-kjpaw_ psl.0.2.3.UPF, Al.pbe-n-kjpaw_psl.0.1.UPF And H.pbe-kjpaw_psl.0.1.UPF from http://www.quantum-espresso.org

[19] Monkhorst H J, Pack J D, Special points for Brillouin-zone integrations, Phys. Rev. B, 1976, 13:5188.

[20] Head J D, Zerner M C, A Broyden-Fletcher-Goldfarb-Shanno optimization procedure for molecular geometries, Chem. Phys. Lett., 1985, 122:264.

[21] Peter E. Blöchl, O. Jepsen, O. K. Andersen, Improved tetrahedron method for Brillouin-zone integrations, Phys.

Rev. B, 1994, 49: 16223.

[22] Chung S., Morioka H., Thermochemistry and crystal structures of lithium, sodium and potassium alanates as determined by ab initio simulations, J. Alloys Compd., 2004, 372: 92.

[23] Lowdin, P. O., On the Non-Orthogonality Problem Connected with the Use of Atomic Wave Functions in the Theory of Molecules and Crystals, 1950, 18: 365.

[24] A. Szabo and N. S. Ostlund, Modern Quantum Chemistry, Dover, 1996.

[25] M. V. Berry, Quantal Phase Factors Accompanying Adiabatic Changes, Royal Society A, 1984, 392: 45.

[26] Mulliken, R. S., Electronic Population Analysis on LCAO-MO Molecular Wave Functions, The J. Chem. Phys,1995, 23(10): 1833.

[27] Vajeeston, P.; Ravindran, P.; Kjekshus, A.; Fjellvag, H., Theoretical modeling of hydrogen storage materials: Prediction of structure, chemical bond character, and high-pressure behavior, J. Alloys Compd. 2005, 77: 404.

[28] O. M. Løvvik , P. N. Molin, Density-functional band-structure calculations of magnesium alanate $Mg(AlH_4)_2$, Phys. Rev. B, 2005, 72: 073201.

[29] Becke, A. D., Edgecombe, K. E., A simple measure of electron localization in atomic and molecular systems, J. Chem. Phys., 1990, 92: 5397.